

EFFECT OF SURFACE ASPERITY TRUNCATION ON THERMAL CONTACT CONDUCTANCE

Fernando H. Milanez^{*}, M. M. Yovanovich[†], J. R. Culham[‡]
 Microelectronics Heat Transfer Laboratory
 Department of Mechanical Engineering
 University of Waterloo
 Waterloo, Ontario, Canada, N2L 3G1
 Phone: (519) 888-4586
 Fax: (519) 746-9141
 E-mail: milanez@mhtlab.uwaterloo.ca

ABSTRACT

This paper presents studies on thermal contact conductance at light contact loads. Surface profilometry measurements are presented which show that actual surface asperity height distributions are not perfectly Gaussian. The highest asperities are truncated, leading the existing thermal contact conductance models to underpredict experimental data. These observations have been incorporated into modifications of existing contact conductance models. The preliminary model has been compared against thermal contact conductance data presented in the open literature, and good agreement is observed. The truncation leads to an enhancement of thermal contact conductance at light contact pressures. The truncation is a function of the roughness level: the rougher the surface, the more truncated the surface height distribution.

KEY WORDS: light contact pressures, truncated Gaussian model, bead blasted surfaces, mean separation gap

NOMENCLATURE

<i>A</i>	contact area, m ²
<i>a</i>	mean contact spot radius, semi-major elliptic contact spot axis, m
<i>b</i>	semi-minor elliptic contact spot axis, m
<i>C_c</i>	dimensionless contact conductance (Eq. 17)
<i>c₁</i>	Vickers microhardness correlation coefficient, Pa
<i>c₂</i>	Vickers microhardness correlation coefficient
<i>E</i>	Young's modulus, Pa
<i>E_ε</i>	equivalent Young's modulus, Pa, (Eq. 4)
<i>H_c</i>	plastic contact hardness, Pa
<i>h_c</i>	contact conductance, W/m ² K
<i>k_s</i>	harmonic mean thermal conductivity, W/mK = $2k_A k_B / (k_A + k_B)$
<i>m</i>	mean absolute roughness profile slope
Nb	Niobium
Ni	Nickel

<i>n</i>	density of contact spots, m ⁻²
<i>P</i>	apparent contact pressure, Pa
<i>p</i>	probability density function
SS	Stainless Steel
<i>v</i>	minimum to maximum slope ratio, (= m_{min}/m_{max})
<i>Y</i>	mean planes separation, m
Zr	Zirconium

Greek symbols

<i>f</i>	thermal constriction factor
<i>l</i>	normalized mean planes separation, m, (= Y/S)
<i>n</i>	Poisson's ratio
<i>s</i>	RMS of surface roughness, m

Subscripts

<i>A, B</i>	contacting bodies
<i>a</i>	apparent
<i>r</i>	real
<i>mn</i>	minimum
<i>mx</i>	maximum
<i>trunc</i>	truncation
<i>TG</i>	Truncated Gaussian model

INTRODUCTION

Since actual surfaces present deviations from their idealized geometrical form, known as roughness and waviness, when two solids are put into contact they will touch only at their highest asperities. The heat transfer across the interface of real solids is not as effective as if the solids were perfectly smooth and flat. A resistance to heat flow, known as thermal contact resistance, appears at the interface between solids. Heat transfer across the interface between two solids has been the subject of study by various researchers over many years. Contact heat transfer has many applications in engineering, such as ball bearings, microelectronic chips and nuclear fuel elements.

When two solids are pressed together, the contacting asperities will deform and form small spots of solid-solid contact. In the remaining portion of the apparent contact area the bodies are separated by very thin gaps. Heat transfer between two contacting solids can take place by three different modes: conduction through the contact spots, radiation through the

^{*} Research Assistant, milanez@mhtlab.uwaterloo.ca

[†] Distinguished Professor Emeritus,

mmyov@mhtlab.uwaterloo.ca

[‡] Associate Professor, Director MHTL,

rix@mhtlab.uwaterloo.ca

gap in the remaining part of the apparent area and conduction through the gas that fills the gap. These heat transfer modes are treated separately and the sum of the conductances associated with each of these heat transfer modes is called joint conductance.

This work is focused on the contact conductance, which is due to conduction through the contact spots. A thermal contact conductance model is generally composed of three models: thermal, geometrical and mechanical deformation models. The thermal model predicts the contact conductance for a given set of contact parameters: shape, size and number of contact spots. These contact parameters are obtained from a particular mechanical deformation model, which can be elastic, plastic or elastoplastic. The deformation model requires a geometric model of the surface in order to be able to predict the contact parameters.

Since it is extremely difficult to predict or to characterize the geometry of actual surfaces by deterministic means, statistical analysis has been generally employed. It is commonly assumed that the surface heights of actual surfaces follow the Gaussian distribution. The Gaussian height distribution model has been used in several thermal contact conductance models, such as the Cooper et al. [1] and the Greenwood and Williamson [2] models, as well as a number of other models derived from these two. It has been reported in the literature [3-6] that these thermal contact models tend to underpredict experimental data at light contact pressures, and as the pressure increases the models and measurements agree. The cause of this behavior was unclear up to now and this subject is addressed here. This work presents evidence that the cause for the models to underpredict the experimental data at light contact pressures is the truncation of the highest asperities. The Gaussian model fails to predict accurately the contact parameters at light contact pressures. A new surface geometric model, called Truncated Gaussian, is proposed here. Modifications are incorporated to the well-established thermal contact conductance models in order to take into account the truncation of the height distribution of actual surfaces.

The next section provides a review of some of the thermal contact conductance models available in the literature. After that, the asperity truncation problem is identified and the new models are presented. The new models are compared against experimental data available in the literature.

REVIEW OF EXISTING MODELS

Most of the thermal contact conductance models available in the literature employ the same thermal model. Cooper et al. [1] first presented the solution for the thermal part of the contact conductance problem. They developed a thermal model for the contact between conforming isotropic rough surfaces, such as those obtained by lapping and bead blasting. The contact between surfaces possessing these features generates approximate circular contact spots randomly distributed over the apparent contact area. The thermal contact conductance between conforming isotropic rough surfaces is given by [1,8]:

$$h_c = \frac{2k_s n a}{\left(1 - \sqrt{A_r/A_a}\right)^{1.5}} \quad (1)$$

where n is the density of contact spots per unit apparent area, a is the mean contact spot radius and A_r/A_a is the real-to-apparent contact area ratio. The term in the denominator of the expression above is called the thermal constriction factor and takes into account for the constriction resistance of the heat flow near the contacting spots. DeVaal [7] extended the Cooper et al. [1] isotropic model to the contact between anisotropic surfaces, such as those obtained by grinding. The contact between such surfaces present elliptical spots rather than circular. The thermal contact conductance between conforming anisotropic rough surfaces is given by:

$$h_c = \frac{k_s n \sqrt{p a b}}{2 f(v, A_r/A_a)} \quad (2)$$

where a and b are respectively the mean semi-major and semi-minor axis of the elliptic contact spots, f is the thermal constriction factor and v is the ratio between the minimum and the maximum slopes of the surface $v = m_{min}/m_{max}$. DeVaal [7] presents the expressions to compute the thermal constriction factor f in detail.

The contact parameters a , b , n and A_r/A_a , appearing in Eqs. (1) and (2), are obtained from the surface geometry and the deformation models. By assuming that the surface heights and slopes are independent and follow the Gaussian distribution, as well as assuming that the surfaces undergo plastic deformation, Cooper et al. [1] presented an analysis to derive expressions for the contact parameters. Yovanovich [8] presented the contact parameter expressions for the isotropic plastic model in a more convenient form. Mikic [9] extended the Cooper et al. [1] plastic model for the case of elastic deformation by assuming that the asperities are spherical near the tips and using results from the Hertz elastic contact theory. DeVaal [7] developed the contact parameter expressions for the contact between anisotropic surfaces under plastic deformation. The expressions for the contact parameters for all these models are shown in Table 1.

The dimensionless plastic contact pressure P/H_c appearing in Eq. (8) of Table 1 can be computed using the model proposed by Song and Yovanovich [10]:

$$\frac{P}{H_c} = \frac{\hat{c}}{\hat{c}_1} \frac{P}{(1.62S/m)^{c_2}} \frac{1}{\hat{u}^{1+0.071c_2}} \quad (3)$$

The equivalent Young's modulus E^c appearing in Eq. (9) of Table 1 is:

$$E^c = \frac{\hat{c}}{\hat{c}_1} \frac{1 - u_A^2}{E_A} + \frac{1 - u_B^2}{E_B} \frac{\hat{c}}{\hat{c}_1} \quad (4)$$

Sridhar and Yovanovich [5] made an extensive review of the thermal contact conductance models available in the literature. Most of the models showed similar results as the models reviewed in this section. The authors also compared the models against experimental data and concluded that the models based on the Cooper et al. [1] model, presented in this section, are very accurate especially at high contact pressures. At light loads, the models tend to underpredict the experimental data. In the next section, it will be shown that the assumption of Gaussian asperity height distribution leads to underestimation of thermal contact conductance at light contact loads. A new model, called Truncated Gaussian model, is proposed here as the modified geometry model.

Table 1. Contact Parameter Expressions

Surface	Contact Parameters
Isotropic	$n = \frac{1}{16} \frac{\pi m \bar{\sigma}^2}{\epsilon^2 s \theta} \frac{\exp(-l^2)}{\operatorname{erfc}(l/\sqrt{2})} \quad (5)$
	$a = \frac{2\sqrt{k}}{\sqrt{p}} \frac{s}{m} \frac{\pi l^2 \bar{\sigma}}{\epsilon^2 2 \theta} \operatorname{erfc} \frac{\pi l \bar{\sigma}}{\epsilon \sqrt{2} \theta} \quad (6)$
	$l = Y/s = \sqrt{2} \operatorname{erfc}^{-1}(2 A_r/A_a) \quad (7)$
	$A_r/A_a = \begin{cases} \frac{1}{2} P/H_c & \text{for plastic} \\ \frac{1}{2} \sqrt{2} P/m\epsilon c & \text{for elastic} \end{cases} \quad (8)$
	$k = \begin{cases} \frac{1}{2} & \text{for plastic} \\ 1 & \text{for elastic} \end{cases} \quad (10)$
Anisotropic (plastic deformation only)	$n = \frac{1}{16} \frac{\pi m \bar{\sigma}^2}{\epsilon^2 s \theta} \frac{\exp(-l^2)}{\operatorname{erfc}(l/\sqrt{2})} \quad (11)$
	$a = \frac{2\sqrt{2}}{\sqrt{p}} \frac{s}{m_{mn}} \frac{\pi l^2 \bar{\sigma}}{\epsilon^2 2 \theta} \operatorname{erfc} \frac{\pi l \bar{\sigma}}{\epsilon \sqrt{2} \theta} \quad (12)$
	$b = \frac{2\sqrt{2}}{\sqrt{p}} \frac{s}{m_{mx}} \frac{\pi l^2 \bar{\sigma}}{\epsilon^2 2 \theta} \operatorname{erfc} \frac{\pi l \bar{\sigma}}{\epsilon \sqrt{2} \theta} \quad (13)$
	$l = Y/s = \sqrt{2} \operatorname{erfc}^{-1}(2 A_r/A_a) \quad (14)$
	$A_r/A_a = P/H_c \quad (15)$

ACTUAL SURFACE HEIGHT DISTRIBUTIONS

The assumption of Gaussian height distribution was first analyzed in more detail by Greenwood and Williamson [2]. They measured surface roughness profiles of bead blasted aluminum surfaces and concluded that the Gaussian distribution is a good approximation at least in the range of surface heights between $\pm 2s$, where s is the RMS of the heights of the profile.

Figure 1 shows measured surface height distributions obtained from three different profiles of a typical bead blasted SS 304 surface. The Gaussian model is also plotted in this graph and it is in good agreement with the measurements for surface heights in the range, especially in the range of $1.5 \epsilon/z/s \leq 3.7$. In typical engineering applications, the mean separation between the contacting surfaces lies in this range. If this surface is brought into contact with a flat lapped surface, for instance, under a contact pressure of $P/H_c=10^{-6}$, which is a very light contact pressure, one can use Eqs. (7) and (8) to calculate a mean separation gap of $Y@4.7s$, according to the Gaussian geometry model. However, the measured profile height distributions do not show asperities higher than $3.7s$. The profile height distributions follow the Gaussian distribution up to $z@3.7s$, where they are truncated. This is expected to be the maximum mean plane separation under the lightest contact load. Therefore, the Gaussian model seems to overpredict the mean plane separation under these circumstances. Since the actual mean plane separation is smaller than predicted by the Gaussian model, the actual thermal contact conductance will be larger than predicted.

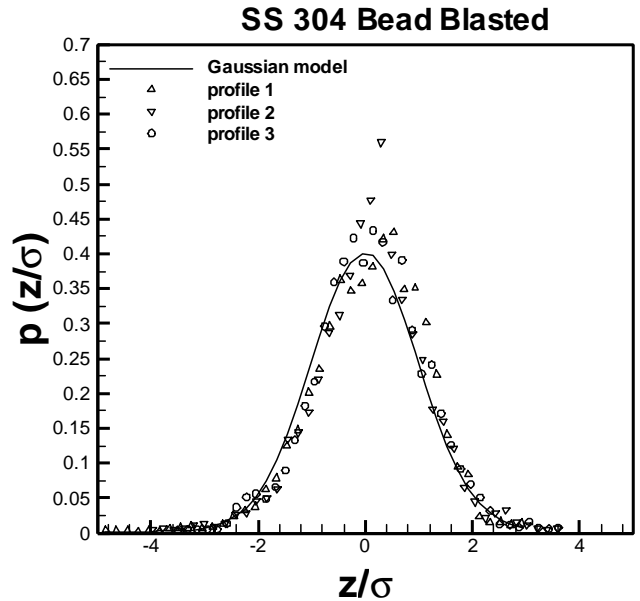


Fig. 1: Measured height distributions of three different profiles of a SS 304 bead blasted surface and comparison with the Gaussian model

Several other researchers [6, 7, 11, among others] also measured profile height distributions of actual machined surfaces and concluded that the Gaussian model is a good approximation. They presented actual surface profile height measurements truncated between 3 and $4s$, but they did not observe the truncation. Only Song [11] identified the consequences of the asperity truncation on the contact conductance problem. He studied the gap conductance problem and proposed a modified expression to compute the mean plane separation between the contacting surfaces.

This expression was derived assuming that the asperity height distribution follows the Gaussian model but is truncated at some height level, called here I_{trunc} . The modified expression for the mean plane separation I_{TG} is written in the following form:

$$I_{TG} = \frac{Y_{TG}}{s} = \sqrt{2} \operatorname{erfc}^{-1} \left(\frac{A_r}{A_a} \right) + \operatorname{erfc} \left(\frac{I_{trunc}}{\sqrt{2}} \right) \quad (16)$$

where, TG stands for Truncated Gaussian and I_{trunc} is the normalized height above which the Gaussian distribution is truncated. Therefore, I_{trunc} is the height of the highest (truncated) asperities, while I_{TG} is the separation between two surfaces in contact according to the Truncated Gaussian model. When the real-to-apparent area ratio A_r/A_a is small, that is, the contact pressure is small (approximately less than 10^{-4}), the second term between the square brackets of Eq. (16) has the same order of magnitude as A_r/A_a . That means that the truncation of the asperities is very important below this contact pressure level. As the contact pressure increases A_r/A_a becomes much larger than $\operatorname{erfc}(I_{trunc}/\sqrt{2})$, and Eq. (16) can be approximated by Eqs. (7) and (14), which represent the fully Gaussian model. Physically, this means that as the pressure increases, more and more asperities come into contact, and as a consequence, the effect of the very few truncated asperities becomes negligible.

Song [11] used Eq. (16) in his gap conductance model and when he compared the results against experimental data he observed good agreement. However, when he tried to use the modified mean plane separation expression to predict contact conductance data, the results of the TG model were much worse than the fully Gaussian model. The present authors now believe that Song [11] was not successful in applying the TG geometry model in the contact conductance model because he used the same expression for the mean contact spot radius as the fully Gaussian model (Eq. 6). A new expression for the mean contact spot radius is proposed in this work and is presented in the next section.

TRUNCATED GAUSSIAN CONTACT CONDUCTANCE MODEL

The asperity height distributions shown in Fig. 1 were obtained from a bead blasted surface, but the authors also analyzed ground and lapped surfaces and found that the results were very similar to bead blasted surfaces: the distributions

were truncated at some height level between 3 and $4s$, approximately. These commonly employed machining processes do not generate asperities higher than this level. The reason for this is still unclear.

In the Truncated Gaussian model, it is assumed that the higher asperities are shorter than predicted by the fully Gaussian model, but they are not missing. The total number of asperities remains the same, although the highest asperities are truncated. Based on this model, the expression for the contact spot density n , Eqs. (5) and (11), are still valid. The correct expression to compute the mean separation gap is now Eq. (16), instead of Eqs. (7) and (14). Also, the mean contact spot radius a (Eq. 6) must be corrected using the following expression:

$$a_{TG} = a \sqrt{1 - \frac{\operatorname{erfc}(I_{trunc}/\sqrt{2})}{\operatorname{erfc}(I_{TG}/\sqrt{2})}} \quad (17)$$

where a_{TG} is the mean contact spot radius according to the Truncated Gaussian model and a is the mean contact spot radius according to fully Gaussian model (Eq. 6). The expression above was obtained by solving $(np a_{TG}^2 = A_r / A_a)$ for a_{TG} , where A_r / A_a is obtained from Eq. (16). The expressions for the semi-major and semi-minor axes for the mean elliptical contact spot of the anisotropic plastic model, Eqs. (12) and (13), become similar to the above expression. The real-to-apparent contact area ratio, the last required contact parameter is computed in the same way as before (Eqs. 7, 8 and 15) because these expressions are obtained from force balances and do not depend on the geometric model used.

The next section presents a comparison between the TG contact conductance model and experimental data available in the literature.

COMPARISON BETWEEN TG MODEL AND EXPERIMENTAL DATA

Hegazy [4] collected a large quantity of thermal contact conductance data between lapped and bead blasted specimens of SS 304, Ni 200, Zr-4 and Zr-Nb possessing various roughness levels. He compared his data with the Cooper et al. [1] isotropic plastic model and noticed that at light contact pressures the model underpredicts the data for all the materials and roughness levels tested. He proposed an explanation for this unexpected behavior as being a consequence of thermal strain and flatness deviations of the test specimens. However, he clearly stated that this explanation was not definitive and further work was needed to clarify this phenomenon. This issue is addressed here and is explained in the light of the new Truncated Gaussian geometric model.

Figures 2 through 4 show the thermal contact conductance experimental data obtained by Hegazy [4] for different metals and different roughness levels. The TG model is also plotted in these graphs as a set of curves for different truncation levels

I_{trunc} because Hegazy [4] did not provide information about the surface height distribution truncation level of his test specimens. The plots show the dimensionless thermal contact conductance C_c as a function of dimensionless contact pressure P/H_c . The dimensionless contact pressure was computed using Eq. (3), and the dimensionless contact conductance is defined as:

$$C_c = \frac{h_c s}{k_s m} \quad (18)$$

The lowest curve of each graph is for $I_{trunc}=+\infty$, which is equivalent to the fully Gaussian model. For practical purposes, a value of $I_{trunc}=5$ is sufficient for the TG model to coincide with the fully Gaussian model. The curve for the fully Gaussian model appears as a straight line in the log-log plots. The curves for the TG model for $I_{trunc}<5$ are concave: they lie above the fully Gaussian model at light contact pressures and tend to the fully Gaussian model as the contact pressure increases. The higher the truncation level (smaller I_{trunc}), the larger the departure of the TG model from the fully Gaussian model. The TG model seems to predict the experimental data trend very well. The experimental data lie between the curve of $I_{trunc}=3.4$ and the curve of the fully Gaussian Model ($I_{trunc}=+\infty$).

LEVELS OF TRUNCATION OF REAL SURFACES

Figure 5 shows a graph of the values of I_{trunc} that best fit Hegazy's [4] data as a function of s/m . Different I_{trunc} are observed for distinct metals possessing the same s/m , although in general I_{trunc} decreases with s/m . The values of I_{trunc} for different metals are scattered between 3.5 and 4.5 for small s/m and tend to approximately 3.5 for large s/m .

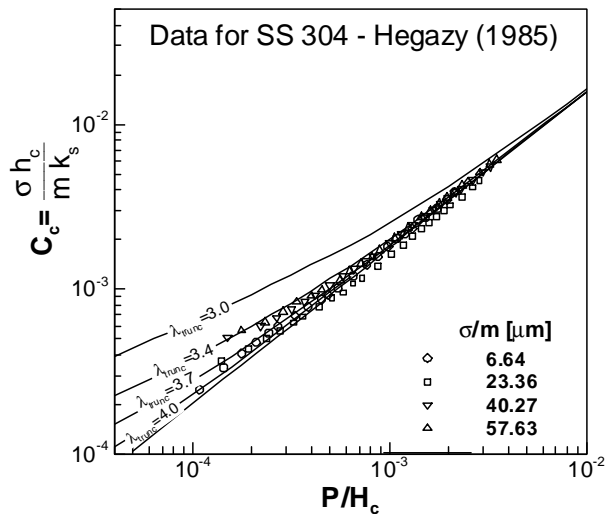


Fig. 2: Thermal contact conductance data for SS 304 from Hegazy [4] and comparison against the TG model

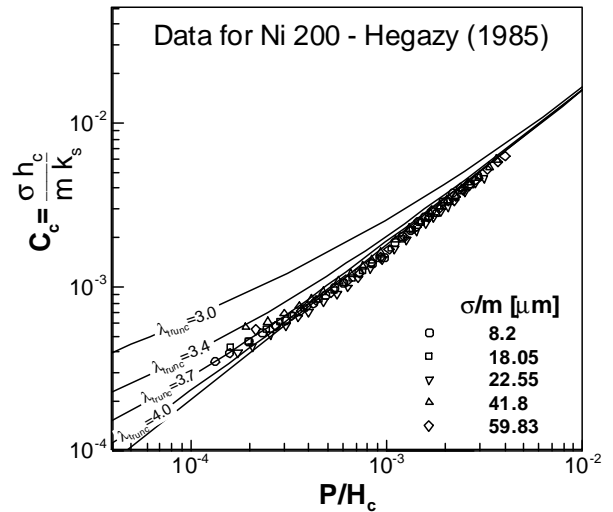


Fig. 3: Thermal contact conductance data for Ni 200 from Hegazy [4] and comparison against the TG model

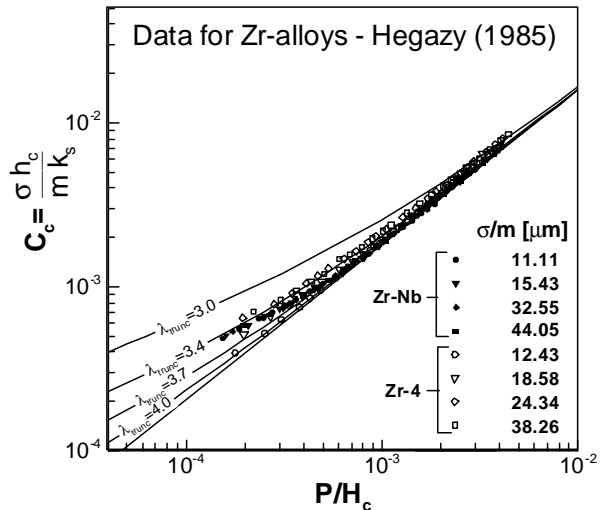


Fig. 4: Thermal contact conductance data for Zr-alloys from Hegazy [4] and comparison against the TG model

The question now is how to predict I_{trunc} for different metals and for different roughness levels? Given the difficulty in modeling analytically the bead blasting process or any other machining process, it seems very difficult to predict I_{trunc} theoretically. Another option is to measure I_{trunc} using a profilometer, the same equipment used to measure s and m . Most of the profilometers available commercially measure a roughness parameter that represents the height of the highest peak of the profile, generally known as R_p [mm]. Song [11] used the R_p collected from a single profilometer trace as a measure for the truncation ($I_{trunc}=R_p/s$). However, it looks

very unlikely that a single trace is able to pass through the peak of the highest asperity of the surface. On the other hand, if one decides to take several different profiles and one of the traces comes across an asperity much higher than the others, this single asperity could not represent the truncation level of the entire surface either because one single asperity can not support the entire contact load alone, even a very light contact load.

In an effort to better understand the truncation of real surface height distributions, the authors decided to undertake a more detailed study of the surface generation process. The authors chose the bead blasting process for this study for various reasons. One can start from a flat lapped surface and by bombarding the surface with glass beads at high speeds, one can “grow” the asperities on the surface at practically any desired RMS roughness level (R_q).

Several bead blasting parameters, such as bead size, air pressure and exposure time can be adjusted in order to generate the desired roughness level. Moreover, this process has been applied very successfully by other thermal contact resistance researchers [3, 4, 6, 11, among others] to generate randomly distributed asperities on the surface without affecting its flatness, which is very important in order to guarantee that the surface geometry is in accordance with the geometric model.

Truncation of bead blasted surfaces

The bead blasting study consisted of measuring the roughness parameters R_p (maximum profile height), s (profile height RMS) and m (profile mean absolute slope) as well as the general trend of the asperity height distribution as a function of bead blasting exposure time between 1 and 16 minutes. Three different blasting pressures (10, 20 and 40 psi) and three different glass bead size ranges (125-180 μm , 279-420 μm and 590-840 μm) were used. Four profiles were assessed over each generated surface, resulting in a total of 136 profile measurements. The minimum and maximum s/m ratios measured during the tests were 12 and 44, respectively. The first important conclusion from this study was that the general trend of the surface height distribution was Gaussian independent of the blasting parameter combinations analyzed. Both the profile height RMS (s) and mean absolute slope (m) as well the ratio s/m increase with increasing exposure time and blasting pressure, as expected, especially for the smaller glass beads. For the largest bead size range tested, the exposure time did not significantly affect either s or m . The blasting pressure was found to be the most important parameter in determining the roughness level.

The main goal of the bead blasting study was to analyze the truncation levels of the surface height distributions for every combination of blasting parameters. It was found that the measured R_p/s (normalized maximum profile height) presented very different values for different profiles collected from the same surface. The largest R_p/s difference measured from different profiles on a single surface was more than 100%. The variation between R_p/s values measured on the

same surface was much larger than the variation between the mean values of R_p/s from different surfaces. Also, the average of the four R_p/s readings on each surface varied randomly among different surfaces. In other words, the R_p/s ratio seemed not to be controlled by any of the bead blasting parameters.

The authors then decided to verify whether the measured R_p/s values could be related to the roughness level of the surface, as observed from the comparison between the TG model and the experimental data [4], independent of the blasting parameters employed. Figure 6 shows a plot of all 136 measured R_p/s values as a function of s/m for all combinations of blasting parameters analyzed. The R_p/s values lie in a large band, which seems to become narrower as s/m increases. The mean value of R_p/s also seems to experience a slight decrease with increasing s/m . These observations are in accordance with the previous conclusion from the comparison between the TG model and the thermal data from Hegazy [4] that I_{trunc} decreases with increasing s/m (Fig. 5). Also, the observation from the thermal tests that I_{trunc} is larger than 3.5 also is consistent with the R_p/s measurements presented in Fig. 6.

The question of how to predict I_{trunc} from roughness measurements still remains unanswered. However, it is clear that a single profile measurement is not sufficiently accurate to measure I_{trunc} because there are only a few truncated asperities and the probability of a single profile trace capture at least one of the truncated asperities is very small. As it can be see from Figs. 2 through 4, the TG model is very sensitive to the value of I_{trunc} , and the measured R_p/s present large variations for the same surface. The authors believe that the best way to obtain information on the correct truncation level is from thermal contact conductance experiments.

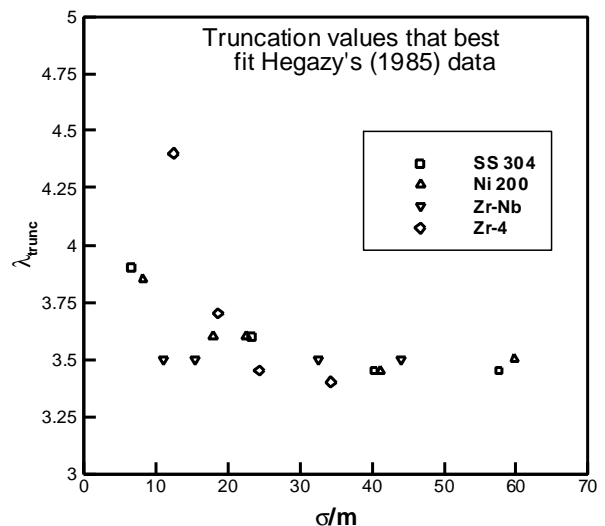


Fig. 5: I_{trunc} values that best fit TG model to experimental data from Hegazy [4] versus s/m

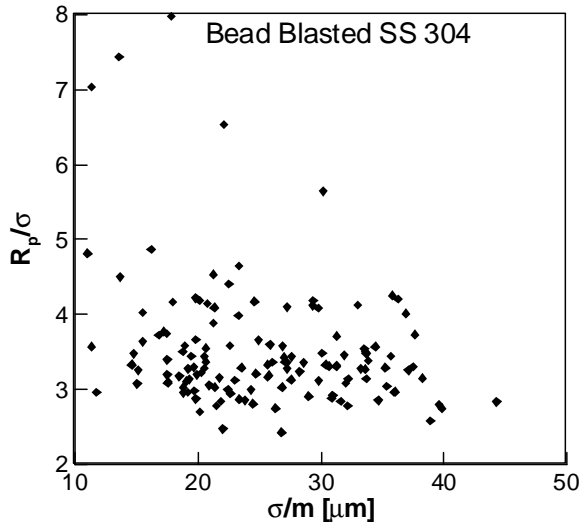


Fig. 6: R_p/s versus s/m for bead blasted SS 304 surfaces

Similar to the method used to obtain the values presented in Fig. 5, by inputting the I_{trunc} value that best fits the TG contact conductance model to the experimental data one can extract information on I_{trunc} . Therefore, more thermal contact conductance data need to be generated for this purpose, especially in the light contact pressure range.

SUMMARY AND CONCLUSIONS

The observation that the existing thermal contact conductance models underpredict experimental data at light contact pressures is reported in several previous thermal contact conductance studies. This work presents evidence that the well-accepted Gaussian surface height distribution geometry model causes the thermal contact conductance models to underpredict the experimental data at light contact pressures. Surface height distribution measurements show that although the distributions follow the Gaussian model for surface heights larger than $1.5s$, the distributions are truncated generally between 3 and $4s$. A new thermal contact conductance model is proposed based on the Truncated Gaussian geometry model. The preliminary results show that the new model predicts the data trend very well. The new model requires another surface parameter, called I_{trunc} , in addition to the parameters s and m . It is not clear at this point how to obtain this third surface parameter from profilometer traces. The use of thermal contact conductance data seems to be the best way to obtain this information.

The truncation of the surface height distribution and its effects on the thermal contact conductance problem is a very important finding but also very recent. Additional studies are needed in order to clarify the questions raised here, especially regarding to the prediction and/or the control of the truncation level of actual machined surfaces.

ACKNOWLEDGEMENTS

The lead author would like to acknowledge the Brazilian Federal Agency for Post-Graduate Education-CAPES for supporting this project. The second and third authors would also like to acknowledge the financial support of the Natural Sciences and Engineering Research Council of Canada.

REFERENCES

- [1] Cooper, M., Mikic, B. and Yovanovich, M. M., "Thermal Contact Conductance," *Journal of Heat and Mass Transfer*, Vol.12, pp. 279-300, 1969.
- [2] Greenwood, J. A. and Williamson, J. B. P., "Contact of Nominally Flat Surfaces," *Proceedings of the Royal Society of London*, pp. 300-319, 1966.
- [3] Milanez, F. H., Culham, J. R., Yovanovich, M. M., "Experimental study on the Hysteresis Effect of Thermal Contact Conductance at Light Loads," 40th AIAA Aerospace Sciences Meeting & Exhibit, January 14-17, Reno, NV, AIAA-2002-0787, 2002.
- [4] Hegazy, A. A., "Thermal Joint Conductance of Conforming Rough Surfaces: Effect of Surface Microhardness Variation", Ph. D. Thesis, University of Waterloo, Ontario, Canada, 1985.
- [5] Sridhar, M. R. and Yovanovich, M. M., "Thermal Contact Conductance of Tool Steel and Comparison with Model," *International Journal of Heat and Mass Transfer*, Vol. 39, No. 4, pp. 831-839, 1996.
- [6] Nho, K. M., "Experimental Investigation of Heat Flow Rate and Directional Effect on Contact Conductance of Anisotropic Ground/Lapped Interfaces," Ph. D. Thesis, University of Waterloo, Ontario, Canada, 1990.
- [7] DeVaal, J. W., "Thermal Joint Conductance of Surfaces Prepared by Grinding," Ph. D. Thesis, University of Waterloo, Ontario, 1988.
- [8] Yovanovich, M. M., "Thermal Contact Correlations," *Spacecraft Radiative Heat Transfer and Temperature Control*, Edited by T. E. Horton, Progress in Astronautics and Aeronautics, Vol. 83, NY, 1981.
- [9] Mikic, B. B., "Thermal Contact Conductance; Theoretical Considerations," *Journal of Heat and Mass Transfer*, Vol. 17, pp. 205-214, Pergamon Press, 1974.
- [10] Song, S. and Yovanovich, M. M., "Relative Contact Pressure: Dependence on Surface Roughness and Vickers Microhardness," *Journal of Thermophysics and Heat Transfer*, Vol. 2, No. 4, pp. 633-640, 1988.
- [11] Song, S., "Analytical and Experimental Study of Heat Transfer Through Gas Layers of Contact Interfaces," Ph. D. Thesis, University of Waterloo, Ontario, 1988.